BIOCHEMISTRY
including biophysical chemistry & molecular biology
Article

Biochemistry **2009,** *48,* 10533–10541 10533
DOI: 10.1021/bi901026z

A Novel Domain in Translational GTPase BipA Mediates Interaction with the 70S Ribosome and Influences GTP Hydrolysis†

Megan A. deLivron, Heeren S. Makanji, Maura C. Lane, and Victoria L. Robinson*

Department of Molecular and Cell Biology, University of Connecticut, Storrs, Connecticut 06269

Received June 17, 2009; Revised Manuscript Received October 1, 2009

ABSTRACT: BipA is a universally conserved prokaryotic GTPase that exhibits differential ribosome association in response to stress-related events. It is a member of the translation factor family of GTPases along with EF-G and LepA. BipA has five domains. The N-terminal region of the protein, consisting of GTPase and β-barrel domains, is common to all translational GTPases. BipA domains III and V have structural counterparts in EF-G and LepA. However, the C-terminal domain (CTD) of the protein is unique to the BipA family. To investigate how the individual domains of BipA contribute to the biological properties of the protein, deletion constructs were designed and their GTP hydrolysis and ribosome binding properties assessed. Data presented show that removal of the CTD abolishes the ability of BipA to bind to the ribosome and that ribosome complex formation requires the surface provided by domains III and V and the CTD. Additional mutational analysis was used to outline the BipA−70S interaction surface extending across these domains. Steady state kinetic analyses revealed that successive truncation of domains from the C-terminus resulted in a significant increase in the intrinsic GTP hydrolysis rate and a loss of ribosome-stimulated GTPase activity. These results indicate that, similar to other translational GTPases, the ribosome binding and GTPase activities of BipA are tightly coupled. Such intermolecular regulation likely plays a role in the differential ribosome binding by the protein.

BipA is a member of the translational family of GTPases (trGTPases)[1] and is required for bacterial survival under adverse environmental conditions (*1*−*6*). Like those of other trGTPases, the biological properties of BipA depend on its GTPase activity as well as its association with the ribosome (*7*−*9*). An examination of the ribosome binding properties of the protein revealed that BipA has two ribosome binding modes (*9*). Under normal growth conditions, BipA interacts with 70S ribosomes in a GTP-dependent manner. However, under conditions of stress, the ribosome binding properties of the protein are altered such that it associates with 30S ribosomal subunits (*9*). Although certain conclusions about these BipA−ribosome complexes can be inferred from comparisons with other members of the trGTPase family, the specific manner in which BipA interacts with the either the 70S or 30S ribosomal particles is yet to be determined.

The closest homologues of BipA are EF-G and LepA (*10*). Cryo-EM and biochemical studies indicate that all three proteins bind to the same universal binding site on the 70S ribosome located at the entrance of the intersubunit space (*7*, *11*, *12*). As such, identification of the structural elements in each trGTPase family that contribute to complex formation with the ribosome is important as these associations influence distinct ribosomal events. EF-G promotes the translocation of tRNA and mRNA through the ribosome during the elongation cycle, a process that has been characterized by many groups over the past three decades (reviewed in ref *13*). LepA, also known as EF4, catalyzes the back translocation of the mRNA−tRNA complex, putting the ribosome in a pretranslocational state (*14*). The function of BipA in the cell is distinct from those of both LepA and EF-G (*8*, *14*). BipA is required for bacterial survival under stressful growth conditions such as low temperature and nutrient depletion (*2*, *3*, *15*). In addition, various lines of evidence support BipA's role in virulence events such as the involvement of the protein in the expression of the LEE and EspC pathogenicity genes, the avirulent nature of a BipA null enteropathic *Escherichia coli* strain, and the upregulation of BipA in response to host defense mechanisms in *Salmonella typhimurium* (*1*, *4*, *16*, *17*). More recent data suggest that BipA may be involved in regulating the later stages of translation (*8*).

EF-G, BipA, and LepA all have five domains. Four of these five domains, the N-terminal G domain, the β-barrel domain, and two α/β-domains, are topologically equivalent (Figure 1). The fifth domain in each of these trGTPase proteins is unique. For EF-G, this unique element is domain IV, whereas in LepA and BipA, it is the C-terminal domain (CTD). Structural studies indicate that although their overall shape is similar, the spatial arrangement of the domains within EF-G, BipA, and LepA proteins is different (*18*−*21*). Therefore, even though the gross morphological features of the EF-G, BipA, and LepA families of proteins are similar, they each have distinctive structural attributes.

†This work was supported by an American Heart Association Scientist Development Grant, a National Science Foundation CAREER Award, and a University of Connecticut Research Foundation Award to V.L.R.

*To whom correspondence should be addressed: Department of Molecular and Cell Biology, University of Connecticut, 91 N. Eagleville Rd., Unit 3125, Storrs, CT 06250. Phone: (860) 486-4353. Fax: (860) 486-4331. E-mail: victoria.robinson@uconn.edu.

[1]Abbreviations: trGTPase, GTPase belonging to the translation factor family; CTD, C-terminal domain; GTP, guanosine 5′-triphosphate; ppGpp, guanosine tetraphosphate; GMPPNP, 5′-guanylyl imidodiphosphate; IPTG, isopropyl β-D-thiogalactopyranoside; βME, 2-mercaptoethanol; DTT, dithiothreitol; SHX, serine hydroxamate; TCA, trichloroacetic acid.

Published on Web 10/05/2009

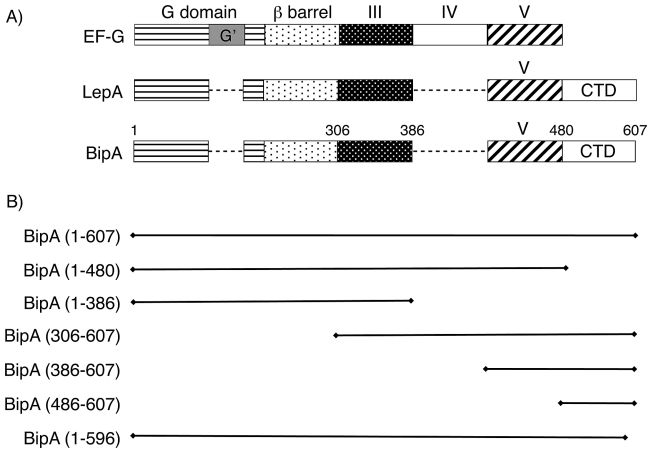

FIGURE 1: Schematic diagram depicting the domain architecture of the EF-G, BipA, and LepA families of trGTPases. (A) Each of these translational GTPases is composed of five individual domains. An N-terminal GTPase or G domain (horizontal stripes), a β-barrel domain (small black dots), and two α/β-domains (larger black dots and diagonal stripes) are common to all three proteins. EF-G has an additional G′ domain (light gray). The unshaded regions, domain IV in EF-G and the C-terminal domains (CTD) in BipA and LepA, are unique to that particular family of GTPases. (B) *Salmonella enterica* BipA protein constructs used in these studies. Locations of the individual domains in BipA have been scaled to the schematic in panel A. The N- and C-terminal truncation constructs were designed as shown. Constructs include full-length BipA(1−607), BipA I−IV-(1−480), BipA I−III(1−386), BipA III-CTD(306−607), BipA IV-CTD(386−607), BipA CTD(486−607), and BipA with the C-terminal basic helix truncated (residues 1−596).

In the following study, we have investigated the contribution of the individual domains of *Salmonella enterica* serovar Typhimurium BipA to the GTPase and ribosome binding activities of the protein. Using a series of deletion constructs, we have demonstrated that the CTD is crucial, but not sufficient, for promoting interaction of BipA with the ribosome. In addition, we have identified key structural elements in the protein required for its association with the ribosome. Chief among these is a highly conserved basic helix at the extreme C-terminus of the protein. We have also established that removal of the CTD results in an increase in the GTPase activity of the protein and the loss of 70S-stimulated GTP hydrolysis activity. Thus, intramolecular contacts in BipA influence the GTPase and the ribosome binding activities of protein. Taken together, these data provide evidence of a functional coupling between the G domain and the CTD, which is potentially utilized in vivo to promote differential association of BipA with the ribosome association in response to environmental conditions.

EXPERIMENTAL PROCEDURES

Cloning and Site-Directed Mutagenesis. N- and C-terminal BipA truncation constructs were generated by polymerase chain reaction (PCR) from *S. enterica* genomic DNA (ATCC 700720D). The resulting DNA fragments encoding domains I−V [BipA(1−480)], domains I−III [BipA(1−386)], domains III, IV, and the CTD [BipA(306−607)], domain V and the CTD [BipA(486−607)], the CTD [BipA(486−607)], and BipA(1−596) were cloned into the *Nde*I and *Xho*I restriction sites of T7 promoter-based expression vector pET28a (Novagen) that adds an N-terminal hexahistidine tag. Site-directed amino acid substitutions were introduced into the full-length N-terminal His-tagged BipA construct by PCR-based site-directed mutagenesis using plasmid pWW3 as a template (*9*). Primers were designed as outlined by Zheng et al. (*22*). Amplification was conducted using Extensor Master Mix (ABgene) in a Techne TC-312 thermocycler. PCR products were digested with *Dpn*I at 37 °C for 45 min and used to transform *E. coli* DH5α cells. Plasmids were confirmed by sequencing at the DNA Biotechnology Facility of the University of Connecticut.

Expression and Purification of Recombinant Proteins. Wild-type as well as singly and doubly substituted BipA recombinant proteins were expressed in *E. coli* strain BL21(DE3). Cells were grown at 37 °C in Luria-Bertani medium supplemented with 30 μg/mL kanamycin to midlog phase and induced with 0.5 mM isopropyl β-D-thiogalactopyranoside (IPTG). The cells were grown for an additional 12−15 h at 16 °C and harvested by centrifugation (5000*g* for 30 min at 4 °C). Cells were washed in 200 mM NaCl, 20 mM Tris-HCl (pH 7.5), and 2 mM 2-mercaptoethanol (βME) (buffer A), pelleted by centrifugation, and stored at −20 °C.

Similar purification procedures were followed for wild-type and substituted proteins. All purification was conducted at 4 °C. Cell pellets were resuspended in buffer A and lysed by sonication, and the cellular debris, including unbroken cells, was removed by centrifugation (20000*g* for 30 min at 4 °C). The supernatant was then loaded onto a 10 mL HisTrap FF crude column (GE Biosciences) equilibrated with buffer A containing 20 mM imidazole. Elution of BipA was conducted with a gradient from 0.02 to 0.5 M imidazole in buffer A. His-tagged BipA protein was concentrated to 1.5 mL using an Amicon Ultra-30 Centrifugal Filter Unit (Millipore) and applied to a Superdex 200 16/60 prep grade column (GE Biosciences) equilibrated in buffer A. Fractions were analyzed by sodium dodecyl sulfate−polyacrylamide gel electrophoresis (SDS−PAGE), and those containing protein that was >95% pure were pooled and stored at −80 °C.

S. enterica (ATCC 700720) 70S, 50S, and 30S ribosomal species were purified as described previously (*9*, *23*).

Ribosome Association Assays. Ribosome association assays were conducted as described with minor alterations (*9*). SB300A *S. enterica* cells (*24*) carrying plasmids encoding the individual His-tagged BipA constructs were grown in MOPS medium (*25*) supplemented with 30 μg/mL kanamycin at 37 °C to an OD_{600} of 0.5−0.6 and induced with 0.2% arabinose. Cells were grown for 2 h, harvested, lysed using a French press, and clarified by centrifugation. Approximately 30 A_{260} units of each S30 extract was layered onto a continuous density sucrose gradient in 20 mM Tris-HCl (pH 7.5), 50 mM NH_4Cl, 10 mM $Mg(OAc)_2$, and 1 mM DTT and centrifuged at 96000*g* in a Beckman SW-28 rotor for 7 h at 13 °C. An AKTA-FPLC was used to monitor the gradient at 254 nm to follow rRNA levels. Fractions were precipitated with 10% trichloroacetic acid (TCA), separated by 12.5% SDS−PAGE, and subjected to Western blot analysis using the HisDetector Western Blot Kit (KPL, Inc.) according to the manufacturer's protocol.

To examine the association of the BipA deletion constructs with the ribosome under adverse growth conditions, SB300A cells transformed with plasmids encoding the individual His-tagged BipA constructs were grown in minimal medium supplemented with 30 μg/mL kanamycin at 37 °C to an OD_{600} of 0.5−0.6 and induced with 0.2% arabinose. After 90 min, serine hydroxamate (SHX) was added to a final concentration of 0.1 mM. The addition of SHX inhibits the charging of serine tRNAs triggering the onset of nutrient depletion, a condition known as the stringent response (*26*−*28*). Cells were grown for an

additional 20 min at 37 °C and harvested by centrifugation. Cosedimentation of BipA with ribosomal particles was examined by Western blotting as described above.

Pelleting Assays. Pelleting assays were performed as described previously (*29*). In brief, 100 pmol of 70S ribosomes was incubated with 100 pmol of His-tagged BipA and 10 mM GMPPNP in 20 mM Tris-HCl (pH 7.5), 200 mM NaCl, 5 mM $Mg(OAc)_2$, and 2 mM DTT for 30 min at 30 °C. Samples (20 μL) were overlaid onto a 2.2 mL sucrose cushion consisting of 1.1 M sucrose, 20 mM Tris-HCl (pH 7.5), 20 mM $Mg(OAc)_2$, 50 mM NH_4Cl, and 10 mM GMPPNP and centrifuged at 250000*g* for 150 min at 4 °C in a S55-A rotor (Sorvall). The supernatant was removed, and the pellets were dissolved in 1 mL of 10 mM Tris-HCl (pH 7.5), 10 mM $Mg(OAc)_2$, 30 mM NH_4Cl, and 1 mM DTT. Supernatant (S) and pellet (P) fractions were precipitated with TCA and resuspended in 200 μL of 2× SDS−PAGE loading buffer, and 25 μL was loaded onto a 12.5% SDS−PAGE gel. The presence of BipA was visualized by Western blotting as described.

GTP Hydrolysis Assays. The GTP hydrolysis activity of the various BipA protein contructs was determined using the malachite green−ammonium molybdate assay described by Lanzetta et al. (*30*). His-tagged BipA proteins (1 μM) were incubated for 5−180 min at 37 °C in a 200 μL reaction mixture containing 20 mM Tris-HCl (pH 7.5), 200 mM NaCl, 20 mM $Mg(OAc)_2$, and 2 mM DTT with 10−5000 μM GTP (GE Biosciences). Where indicated, 5 nM purified ribosomal particles were incubated with BipA on ice for 15 min before the addition of GTP. Thirty microliters of the reaction mixture was added to 0.8 mL of the acidic malachite green solution to stop the reaction. After incubation for 30 min at room temperature, color formation was assessed at 660 nm with a DU640 spectrophotometer (Beckman). Kinetic data were analyzed by being fit to the Michaelis−Menten equation with nonlinear regression curve fitting using GraphPad Prism version 4.0 (GraphPad Software Inc.). Reported results correspond to at least three independent experiments. Background GTP hydrolysis rates were measured for the isolated ribosome species.

Circular Dichroism Measurements. Circular dichroism spectra were recorded using an Applied Photophysics Pi-Star 180 spectropolarimeter with the cuvette maintained at 20 °C with a circulating water bath. All protein samples were at a concentration of 1 mg/mL in 20 mM sodium phosphate and 100 mM NaCl (pH 7.5). Spectra were recorded under nitrogen with a 0.1 cm path length. Samples were evaluated every 1 nm from 200 to 250 nm with entrance and exit slit widths of 2 nm. Mean residue molar ellipticity was calculated using the formula $[\theta]_{MRW} = \theta/(10c_r l)$, where c_r is the mean residue molar concentration, θ is the ellipticity in millidegrees, and l is the path length in centimeters.

RESULTS

Ribosome Association by BipA Requires the CTD. The functional roles of the individual domains in BipA have yet to be established. To examine the contribution of each domain to the GTPase and ribosome binding activities of the protein, a series of N- and C-terminal BipA deletion constructs were designed on the basis of domain boundaries defined from amino acid sequence alignments and from the partial crystal structure of BipA from *Vibrio parahemolyticus* [Protein Data Bank (PDB) entry 3E3X] (Figure 1A). The nomenclature designates which amino acids are present in the construct; i.e., BipA(1−480) consists of the first four domains of the protein. The role of the C-terminal domain of BipA was of great interest. We believe this domain, which is unique to the BipA family of GTPases, serves as a specificity element to functionally distinguish BipA from closely related translational GTPases such as EF-G and LepA.

Each truncation construct was assessed for ribosome binding under normal growth conditions as described in Experimental Procedures (Figure 2A). In agreement with previous data, full-length BipA cofractionated with the 70S ribosome (*7*, *9*). In contrast, the BipA(1−386) and BipA(1−480) proteins remained at the top of the gradient, free in solution, indicating that the surface supplied by the CTD is a necessary component of the 70S−BipA ribosome interface. We also observed that the isolated CTD does not associate with any ribosomal species and thus is required, but is not sufficient, for BipA to bind to the ribosome. Two N-terminal deletion constructs were also assessed. BipA(486−607) showed no measurable ribosome binding, whereas BipA(306−607) associated with 70S ribosomes.

It was previously demonstrated that when bacteria are experiencing nonoptimal growth conditions, such as nutritional depletion or temperature stress, the ribosome binding properties of BipA are altered so that it associates with 30S ribosomal subunits (*9*). To examine the involvement of the individual domains in the formation of the 30S−BipA complex, ribosome binding by the His-tagged BipA deletion constructs was examined under nutrient-depleted growth conditions caused by the addition of SHX to the cell culture. The results from these experiments are shown in Figure 2B. In agreement with our previous data, under these stringent growth conditions, full-length BipA cosedimented with the 30S ribosomes (*9*). Without the CTD, BipA(1−480) does not associate with any ribosomal species. However, BipA(306−607) was detected in fractions corresponding to 70S ribosomes. The results of the binding experiments for the BipA(1−480) and BipA(306−607) constructs are similar under both normal and adverse growth conditions, suggesting that the surface supplied by domains III, V, and the CTD is necessary for BipA to bind to either the 70S or 30S ribosomal species.

The data from our ribosome binding studies under normal growth conditions suggest that BipA(1−386) may have a higher degree of 70S ribosome association in comparison to the other constructs. We assessed the relative levels of expression for each of the BipA deletion constructs under conditions that matched those used in the ribosome binding studies and then detected BipA in the lysates with our standard His detection Western protocol. Briefly, SB300A cells transformed with a given variant were grown in MOPS medium at 37 °C until midlog phase when the cultures were induced with 2% arabinose. After 2 h, the cells were harvested and an equivalent amount of total soluble lysate from each strain was loaded onto a SDS−PAGE gel and analyzed by Western blotting (Figure 2C). These results show that BipA(1−386) has higher expression levels in comparison to the six other constructs. Therefore, the observed enhancement of 70S binding is due to the higher cellular concentration of this BipA variant.

GTP Hydrolysis by BipA Truncation Constructs. The intrinsic GTP hydrolysis rates of the C-terminal truncation constructs BipA(1−386) and BipA(1−480) were investigated using the malachite green−ammonium molybdate colorimetric assay (*30*) (Figure 3). Both proteins exhibited increased k_{cat} values as compared to that of wild-type BipA. Removal of the CTD increases k_{cat} to $141.7 \pm 7.5\ h^{-1}$ which is approximately

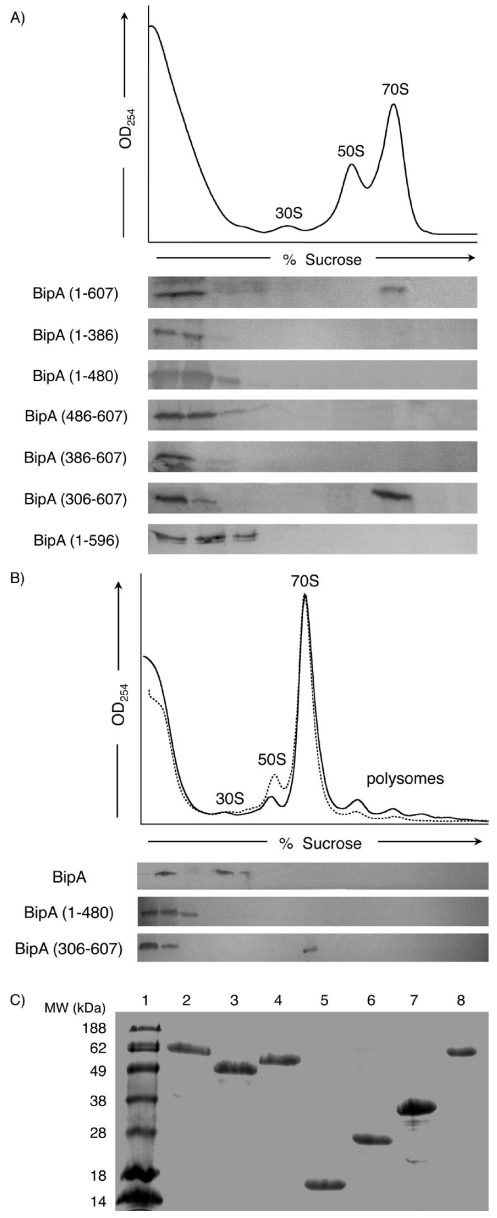

FIGURE 2: Ribosome association profiles of the BipA truncation constructs under normal and nutrient-depleted growth conditions. (A) *S. enterica* SB300A cells containing a plasmid encoding one of the His-tagged truncation constructs described in Figure 1 were grown in MOPS medium at 37 °C to midlog phase and induced with 0.2% arabinose. Two hours after induction, the cells were harvested and lysed with a French press. Clarified lysates were sedimented through a 7 to 47% sucrose gradient, and the ribosome profile was monitored at 254 nm. Individual gradient fractions were precipitated with TCA and analyzed by 12.5% PAGE and Western blotting against the His-tagged BipA. 70S, 50S, and 30S ribosomal species have been labeled. (B) Similar experiments were conducted under conditions of amino acid starvation caused by the addition of SHX. In brief, cells were grown to midlog phase and induced with 0.2% arabinose. After the cells had grown for 90 min, 0.1 mM SHX was added and the cells were grown for an additional 30 min. Cosedimentation of the individual BipA deletion constructs with various ribosomal particles on a 17 to 57% sucrose gradient was assessed as described for panel A. (C) Western blot indicating the level of protein expression for each BipA deletion construct grown in SB300A cells as specified in panel A. The amount of BipA in each cell lysate was determined by loading 0.01 OD_{600} unit onto a 12.5% SDS−PAGE gel and immunoblotting. His-tagged BipA was detected as described above using the HisDetector Western blotting kit: lane 1, molecular mass markers; lane 2, BipA(1−607); lane 3, BipA(1−386); lane 4, BipA(1−480); lane 5, BipA(486−607); lane 6, BipA(386−607); lane 7, BipA(301−607); lane 8, BipA(1−597).

7-fold greater than that determined for the full-length protein, 19.8 ± 0.2 h^{-1} (*9*). BipA(1−386) exhibited an even higher turnover rate, a k_{cat} value of 348.8 ± 28.8 h^{-1}, which is 18-fold greater than the intrinsic GTPase activity of full-length BipA (Figure 3C). This significant increase in the hydrolytic activity of the truncated proteins suggests that intramolecular contacts involving domain V and the CTD contribute to the regulation of the intrinsic GTP hydrolysis rates in the protein. Because the CTD of BipA is crucial for ribosome binding, we predicted that BipA(1−386) and BipA(1−480) should not exhibit ribosome-stimulated hydrolysis activity as is observed for the full-length protein (*7*, *9*). The GTPase activities of BipA(1−480), in the presence of 70S ribosomes, 50S ribosomal subunits, and 30S ribosomal subunits, are 148.4 ± 8.7, 146.5 ± 40, and 159.5 ± 41 h^{-1}, respectively. These values are similar to the intrinsic activity of BipA(1−480) (Figure 3D). The same trend was observed for the BipA(1−386) protein; that is, no significant change in the GTP hydrolysis rate was observed for this construct in the presence of various ribosomal species (data not shown). These data substantiate the importance of the CTD to the ribosome-stimulated GTP hydrolysis activity of BipA.

The Conserved C-Terminal Helix Is Required for Ribosome Association. A BLAST search revealed that the 20 residues at the C-terminus of the protein are conserved across the BipA family. In addition, analysis of the *S. enterica* BipA amino acid sequence with BindN (*31*) and RNABindR (*32*) pinpoints residues 592−605 as possible RNA interaction sites. The last six residues visible in the CTD of the *V. parahemolyticus* BipA structure (595-NDRRRA-600) form a small basic helix extending from the body of the protein (PDB entry 3E3X). Therefore, a construct, BipA(1−596), was designed lacking this C-terminal basic helix and the ribosome association of this BipA construct determined by sucrose density gradient centrifugation as described previously. As shown in Figure 2A, BipA(1−596) remained at the top of the sucrose gradient, indicating that without this helix, BipA is unable to bind to the ribosome.

70S Ribosome Binding Surface of BipA. The following sets of experiments were designed to identify specific areas of BipA important to its association with the ribosome. Residues were chosen on the basis of three primary criteria: sequence conservation in the BipA family (BLAST) (*33*), identification as putative RNA interaction sites as predicted by BindN (*31*) and RNABindR (*32*), and contribution to surface electrostatic potential determined using a model of BipA. The BindN and RNABindR programs are used to predict RNA-binding residues from a given protein sequence. BindN uses support vector machine (SVM) analysis which takes sequence conservation, side chain pK_a, hydrophobicity, and molecular mass into consideration, while RNABindR uses a Naïve Bayes classifier based on interface amino acid propensities and sequence periodicities. The homology model of *S. enterica* BipA was calculated with MODELER (*34*) using the apo LepA (PDB entry 3CB4) and *V. parahemolyticus* BipA (PDB entry 3E3X) atomic coordinates (*21*). The *V. parahemolyticus* BipA structure, which is a partial model consisting of three C-terminal domains, has a sequence 72% identical with that of *S. enterica* BipA residues 301−607. *E. coli* LepA and *S. enterica* BipA share 32.4% amino acid sequence identity. The best fit model of BipA was validated using PROCHECK.

The RNA binding prediction programs identified three potential interaction sites in domain V and the CTD of BipA. These areas consist of residues 422−436 in domain V and residues

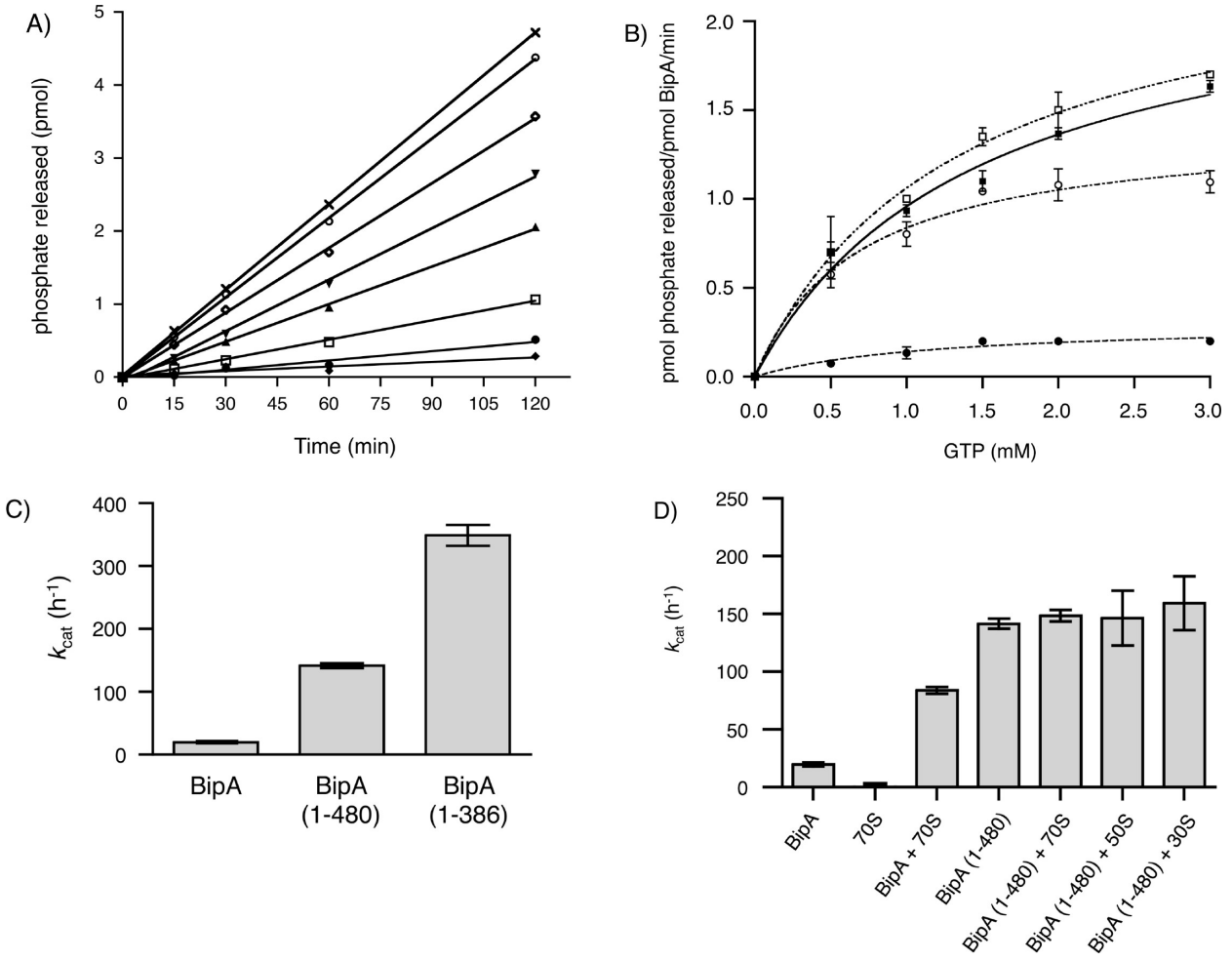

FIGURE 3: Steady state kinetic assays measuring the GTP hydrolysis activities of the N-terminal BipA truncation constructs. (A) Time course of the BipA-catalyzed GTP hydrolysis reactions observed at different starting concentrations of GTP determined using the malachite green−ammonium molybdate assay to measure the amount of phosphate produced from reactions. Reaction mixtures contained 1 μM BipA and 0.05 (◆), 0.1 (●), 0.25 (□), 0.5 (▲), 1.0 (▼), 2.5 (◇), 3.5 (○), and 4.5 mM GTP (×) in 20 mM Tris-HCl (pH 7.5), 200 mM NaCl, 20 mM $Mg(OAc)_2$, and 2 mM DTT. (B) Initial velocity rates were measured for 180 min at 37 °C for reaction mixtures that contained 1 μM protein and GTP concentrations ranging from 0.5 to 3.0 mM. GTP hydrolysis rates of full-length BipA in the absence (●) and presence (○) of 70S ribosomes and of the BipA(1−480) construct in the absence (■) and presence (□) of 70S ribosomes are shown. (C) Bar graph comparing the intrinsic rates of hydrolysis for the BipA N-terminal truncation constructs. The k_{cat} values were determined by fitting the Michaelis−Menten equation using nonlinear regression algorithms furnished with GraphPad Prism (GraphPad Software, Inc.). (D) Ribosome-stimulated GTP hydrolysis is not observed for the BipA(1−480) construct. GTP hydrolysis by BipA(1−480) (1 μM) was assayed with 5 nM 70S ribosomes, 30S ribosomal subunits, or 50S ribosomal subunits in the presence of 1% glycerol using the malachite green assay as described previously. Experiments were conducted in triplicate and k_{cat} values determined. The intrinsic and 70S-stimulated GTP hydrolysis rates for full-length BipA and for 70S ribosomes alone are shown for the sake of comparison.

527−532 and 581−605 in the CTD. Interestingly, no potential RNA interaction sites were predicted for domain III. Consequently, residues chosen to be examined for their contribution to ribosome binding by BipA included R422/K423, K427, and K434/R436 in domain V. In the CTD, two sets of residues were chosen for investigation. These include a basic patch in the proximity of the C-terminal helix formed by R507, H527, and R529 and another set of basic residues on an adjacent face of the CTD that includes R375, K509, and K562. Lastly, we turned our attention to the extreme C-terminus of the protein. We have shown that the C-terminal helix, residues 597−607, of BipA is required for 70S association. Preceding this helix is a β-hairpin structure that forms an extension of the β-sheet in domain III (Figure 4). On one side of this β-sheet is a large loop that extends down from domain III covering one surface of this CTD β-hairpin. E322 and T315 are located at either end of this loop and form ionic interactions with the side chains of R586 and R588, respectively. These strictly conserved arginines likely stabilize the relative positioning of domain III and the CTD, so their contribution to the ribosome binding properties of BipA was also assessed.

The CTD of BipA has a large flexible loop at the distal end of the protein. A similarly positioned loop is present in the EF-G family of proteins (*18*, *19*). Substitutions of residues in this region of EF-G resulted in a dramatic decrease in translocation rates (*35*). Cryo-EM studies later confirmed that this loop is essential to the "induced fit" binding of EF-G to the ribosome (*36*). BipA has four strictly conserved residues in this loop, N536, K541, K542, and R547. Each was replaced with an alanine. In addition, a proline was introduced at position 544 to decrease the overall flexibility of the region.

Alanine substitutions were made for each of the aforementioned residues using site-directed mutagenesis as described in Experimental Procedures. CD spectroscopy was used to evaluate whether the secondary structure of the protein was altered by the introduction of a given amino acid substitution. Representative

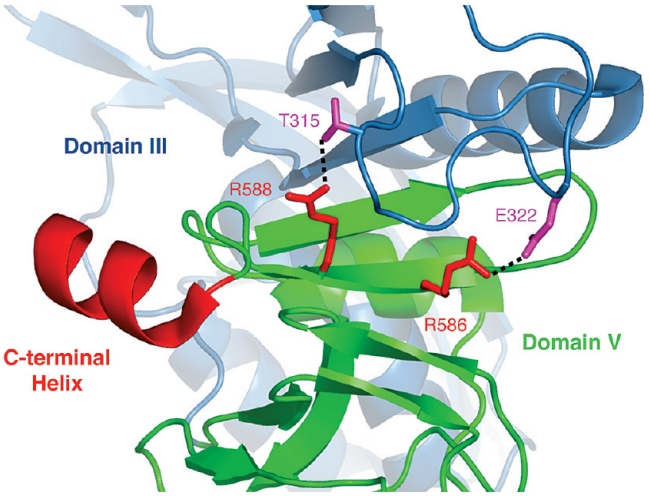

FIGURE 4: Structure of the C-terminal region of BipA. Ribbon diagram of domain III (blue) and the CTD (green) of *S. enterica* BipA modeled from the *V. parahemolyticus* structure (PDB entry 3E3X). The highly conserved basic helix at the extreme C-terminus of the protein is colored red. CTD residues R586 and R588 (red sticks) are positioned at either end of a β-hairpin loop that forms an extension of a large centrally located β-sheet in domain III. On one side of this β-sheet is a large loop that extends down from domain III across the CTD. A pair of strictly conserved ionic interactions between R586 and T315 (magenta sticks) and R588 and E322 (magenta sticks) secure the positioning of this loop. These highlighted interactions are likely involved in stabilizing the position of the domains relative to one another. Figures were generated using PyMOL (*44*) from the BipA homology model.

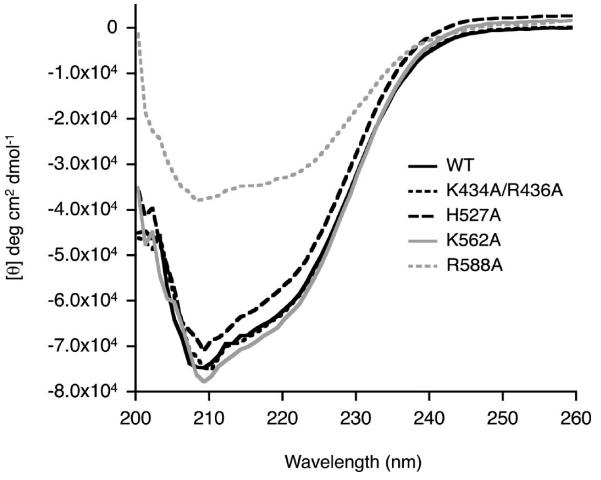

FIGURE 5: Representative CD spectra of the substituted BipA proteins. CD spectra of wild-type (solid line), K434A/R436A (short dashed line), H527A (long dashed line), K562A (gray line) and R588A (gray dashed line) BipA proteins.

spectra are shown in Figure 5. The majority of the mutant constructs exhibited spectra characteristic of wild-type BipA. However, R586A and R588A showed a decrease in the magnitude of the CD signal, indicating a change in the secondary structure of these proteins. Pelleting assays were then used to examine the ribosome binding properties of each BipA protein in the presence of GMPPNP. Fractions corresponding to free BipA (supernatant) and BipA in complex with the ribosome (pellet) were precipitated with TCA, and the presence of BipA in these fractions was analyzed by Western blotting.

The results of the ribosome association experiments with the mutated BipA proteins are shown in Figure 6. In domain V, the K434A/R436A and K427A proteins did not bind to any ribosomal particles. In contrast, the R422A/K423A construct bound to 70S ribosomal species. In the CTD, R507A bound to the 70S ribosome while the H527A, R529A, and K562A BipA constructs did not. Ribosome association was restored when a lysine was substituted for H527, thus establishing the necessity of a positive charge at the center of this cluster for formation of the 70S−BipA complex. The R375A and K509A proteins exhibited 70S ribosome binding, suggesting the loss of positive charge on this face of the CTD had little influence on formation of the 70S−BipA complex. R586A and R588A were not able to bind any ribosomal species. Similarly, all five substitutions in the loop region of the CTD hinder the association of BipA with the ribosome (Figure 6B).

DISCUSSION

In this study, we examined the participation of the individual domains of *S. enterica* BipA in ribosome binding and in the regulation of the GTPase activities of the protein. As mentioned previously, BipA has five domains. Four of these five domains have structural counterparts in EF-G and LepA, whereas the CTD is distinct to the BipA family. From an analysis of the ribosome binding properties of N- and C-terminal BipA deletion constructs, we established that the CTD is crucial in mediating the interaction of BipA with the 70S ribosome but is unable to bind to the ribosome in isolation. Formation of a complex with the 70S ribosome requires a BipA construct containing residues 306−607, revealing that the interaction surface of the protein extends beyond that provided by the CTD domain alone.

Previous studies from our lab suggest that the differential association of BipA with the ribosome is due, at least in part, to the nature of the guanine nucleotide bound to the protein (*9*). We had shown that GTP-bound BipA associates with the 70S ribosome whereas BipA associates with 30S ribosomal subunits in a ppGpp-dependent manner. Data presented here reveal that the CTD is also a necessary component of the 30S−BipA complex formed during adverse growth conditions. Intriguingly, under stringent growth conditions, BipA(306−607) cofractionated with the 70S ribosomes, not with the 30S ribosomal subunits. The absence of the N-terminal GTPase and β-barrel domains prevents differential ribosome association by this construct. This supports the hypothesis that the nucleotide-bound state of the protein contributes to the altered specificity of BipA for a given ribosomal species likely through coordinated conformational changes across the length of the protein.

Additional evidence of intramolecular regulation in BipA comes from measuring the GTP hydrolysis activity of the deletion constructs. Kinetic analysis indicated that the steady state rate of GTP turnover by the BipA(1−480) protein (k_{cat} = 141.7 h^{-1}) is higher than that of full-length BipA either in the presence (k_{cat} = 83.9 h^{-1}) or in the absence of the ribosome (k_{cat} = 19.8 h^{-1}) (*9*). The largest increase in intrinsic GTPase activity was measured for the BipA(1−386) construct ($k_{cat} \sim$ 349 h^{-1}), which was 17-fold higher than the activity of full-length BipA. In addition, none of the C-terminal deletion constructs exhibited ribosome-stimulated GTPase activity, confirming our previous results that the CTD is required for ribosome association. Examination of the BipA model indicates that the switch regions of the G domain are located at the interface among domains I, III, and V. Therefore, the enhanced activity of BipA(1−386) may be a consequence of increased flexibility in the switch regions conferred by the absence

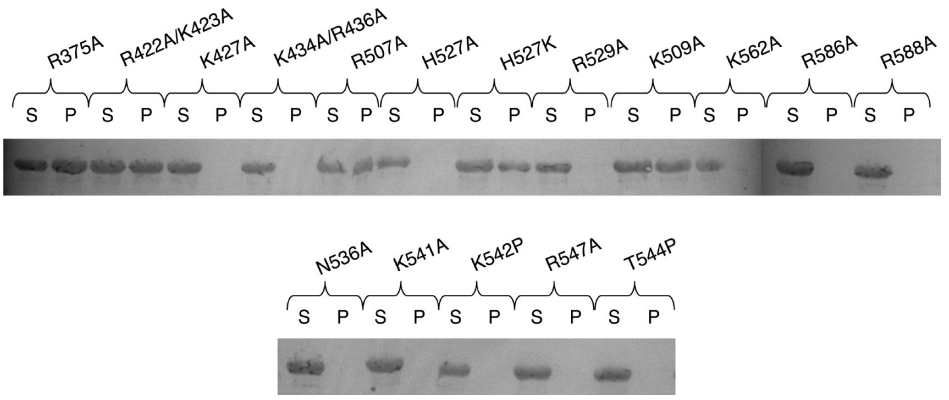

FIGURE 6: Association of the alanine-substituted BipA constructs with 70S ribosomes in the presence of GMPPNP. (A) Binding of BipA to 70S ribosomes was assessed by incubation of equimolar concentrations of ribosomes with a given His-tagged BipA construct in the presence of 20-fold molar excess of GMPPNP at 30 °C for 30 min. The sample was then applied to a 1.1 M sucrose cushion and centrifuged. The supernatant (S) fraction containing free BipA and the pelleted (P) fractions containing protein bound to the ribosome were precipitated with TCA and applied to a 12.5% SDS−PAGE gel, and the presence of BipA in each fraction was detected by immunoblotting using a HisDetector kit. (B) Similar experiments were conducted for BipA mutants with alanine substitutions in the loop region.

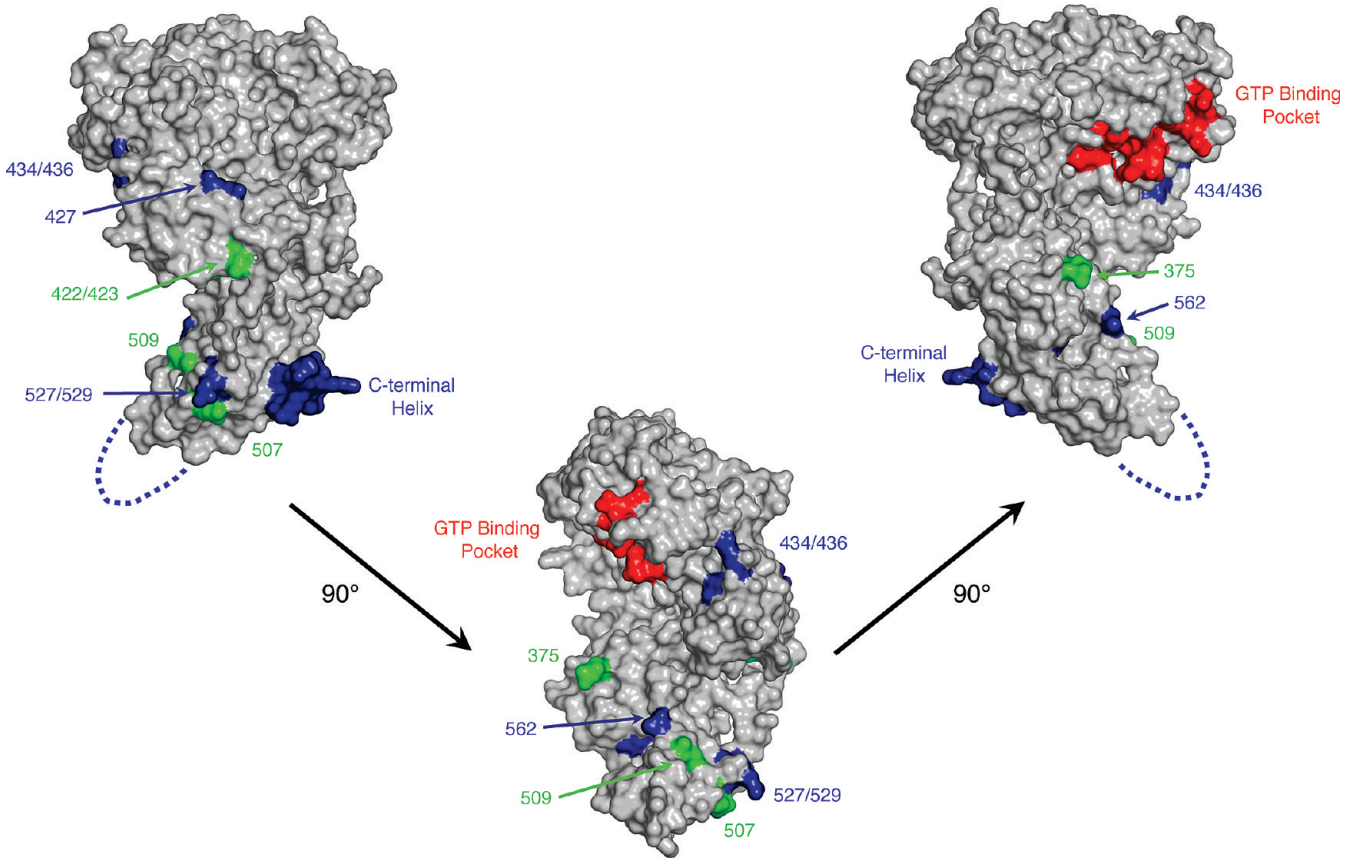

FIGURE 7: Surface representation depicting the structural elements important for 70S ribosome binding by BipA. Results from the ribosome binding experiments mapped onto the surface of the *S. enterica* BipA model. The GTP binding pocket, defined by the conserved G1, G3, and G4 motifs, is colored red. Residues that contribute to 70S ribosome binding, including the flexible CTD loop, are colored blue, while those not essential for ribosome association are colored green. Taken together, these data provide a rough outline of the 70S ribosome-binding surface of BipA. Figures were generated using PyMOL (*44*) from the BipA homology model.

of domain V and the CTD. This does not, however, explain the increase in the rate of GTP hydrolysis observed in the BipA-(1−480) construct. The C-terminal domain does not physically interact with the GTPase domain, so the increase in k_{cat} for BipA(1−480) cannot be explained as a simple relief of inhibition. These data, coupled with the ribosome binding studies mentioned above, suggest that a reciprocal pathway of interdomain allosteric communication between the GTPase and the C-terminal domains modulates the GTPase and ribosome binding properties of the protein.

As shown in Figure 7, we have identified a series of structural features that contribute to 70S binding by BipA. There are several basic patches important for formation of the 70S−BipA complex, one in the CTD and the others spread across the exposed face of domain V. These elements outline a surface on BipA extending from the CTD across the length of protein to the

nucleotide-binding site. Another key structural component required for ribosome binding is a highly conserved basic helix at the extreme C-terminus of the protein. This is interesting as a random deletion of the 11 C-terminal amino acids from *E. coli* BipA negated the ability of the bacteria to colonize the mouse large intestine (*37*). This colonization defect may be due to the inability of BipA to form a stable complex with the ribosome. Data are also presented to indicate that the overall character of the C-terminal region of the protein is essential for ribosome binding. Two strictly conserved arginines, R586 and R588, stabilize the positioning of a long loop from domain III to the CTD (Figure 5). Our CD data indicate that replacement of either R586 or R588 with alanine resulted in increased structural disorder in the protein and the loss of ribosome binding. Interestingly, this loop lies in the proximity of the basic C-terminal helix.

Another prominent structural element in BipA is a disordered loop located at the distal end of the CTD (Figure 7). Replacement of the strictly conserved residues within this region with alanine negates ribosome binding. Likewise, restricting flexibility of the loop with a centrally placed proline abolishes the association of BipA and the 70S ribosome. Domain IV of EF-G, the spatial equivalent of the CTD of BipA, also has two flexible loops in a similar location at the tip of the domain. Cryo-EM structures revealed this loop is positioned at the A-site of the 70S ribosome (*11*, *38*−*41*). Moreover, residues in this region of EF-G domain IV support tRNA translocation (*35*, *42*, *43*). As BipA and EF-G have the same overall morphology and bind to equivalent but not identical sites on the ribosome, it is possible that this flexible loop in BipA occupies a position close to the A-site tRNA, so it is tempting to speculate that BipA stabilizes the A-tRNA and/or occludes the A-site at some point in the translation process.

In summary, this work substantiates the importance of the novel CTD of BipA in the coordinated regulation of ribosome binding and GTP hydrolysis activities of the protein. Foremost, the CTD provides a prominent and distinctive binding surface enabling BipA to interact selectively with a given state of the ribosome. Data presented demonstrate that severing the communication link between the GTPase domain and the C-terminal region of the protein prohibits differential binding of BipA to the ribosome. This supports our previous hypothesis that BipA exists in at least two different states, a GTP-bound form poised to interact with the 70S ribosome and a ppGpp-bound conformation that preferentially binds to the 30S ribosomal subunit (*9*). The relative orientation of the domains in these two states is almost certainly dictated by the nature of the bound guanine nucleotide, a regulatory mechanism employed by many multidomain GTPases, including EF-G and LepA. Ongoing structural studies will provide a mechanistic description of how interdomain communication contributes to the biological properties of the protein.

ACKNOWLEDGMENT

We thank Dr. Jeffrey McKinney for the gift of the SB300A strain and Dr. Carolyn Teschke for input and the use of her CD.

REFERENCES

1. Farris, M., Grant, A., Richardson, T. B., and O'Connor, C. D. (1998) BipA: A tyrosine-phosphorylated GTPase that mediates interactions between enteropathogenic *Escherichia coli* (EPEC) and epithelial cells. *Mol. Microbiol. 28*, 265–279.
2. Pfennig, P. L., and Flower, A. M. (2001) BipA is required for growth of *Escherichia coli* K12 at low temperature. *Mol. Genet. Genomics 266*, 313–317.
3. Beckering, C. L., Steil, L., Weber, M. H., Völker, U., and Marahiel, M. A. (2002) Genomewide transcriptional analysis of the cold shock response in *Bacillus subtilis*. *J. Bacteriol. 184*, 6395–6402.
4. Grant, A. J., Farris, M., Alefounder, P., Williams, P. H., Woodward, M. J., and O'Connor, C. D. (2003) Co-ordination of pathogenicity island expression by the BipA GTPase in enteropathogenic *Escherichia coli* (EPEC). *Mol. Microbiol. 48*, 507–521.
5. Kiss, E., Huguet, T., Poinsot, V., and Batut, J. (2004) The typA gene is required for stress adaptation as well as for symbiosis of *Sinorhizobium meliloti* 1021 with certain Medicago truncatula lines. *Mol. Plant-Microbe Interact. 17*, 235–244.
6. Reva, O. N., Weinel, C., Weinel, M., Böhm, K., Stjepandic, D., Hoheisel, J. D., and Tümmler, B. (2006) Functional genomics of stress response in *Pseudomonas putida* KT2440. *J. Bacteriol. 188*, 4079–4092.
7. Owens, R. M., Pritchard, G., Skipp, P., Hodey, M., Connell, S. R., Nierhaus, K. H., and O'Connor, C. D. (2004) A dedicated translation factor controls the synthesis of the global regulator Fis. *EMBO J. 23*, 3375–3385.
8. Krishnan, K., and Flower, A. M. (2008) Suppression of delta bipA phenotypes in *Escherichia coli* by abolishment of pseudouridylation at specific sites on the 23S rRNA. *J. Bacteriol. 190*, 7675–7683.
9. deLivron, M. A., and Robinson, V. L. (2008) *Salmonella enterica* sv. Typhimurium BipA Exhibits Two Distinct Ribosome Binding Modes. *J. Bacteriol. 190*, 5944–5952.
10. Margus, T., Remm, M., and Tenson, T. (2007) Phylogenetic distribution of translational GTPases in bacteria. *BMC Genomics 8*, 8–15.
11. Agrawal, R. K., Penczek, P., Grassucci, R. A., and Frank, J. (1998) Visualization of elongation factor G on the *Escherichia coli* 70S ribosome: The mechanism of translocation. *Proc. Natl. Acad. Sci. U.S.A. 95*, 6134–6138.
12. Connell, S. R., Topf, M., Qin, Y., Wilson, D. N., Mielke, T., Fucini, P., Nierhaus, K. H., and Spahn, C. M. (2008) A new tRNA intermediate revealed on the ribosome during EF4-mediated back-translocation. *Nat. Struct. Mol. Biol. 15*, 910–915.
13. Frank, J., Gao, H., Sengupta, J., Gao, N., and Taylor, D. J. (2007) The process of mRNA-tRNA translocation. *Proc. Natl. Acad. Sci. U. S.A. 104*, 19671–19678.
14. Qin, Y., Polacek, N., Vesper, O., Staub, E., Einfeldt, E., Wilson, D. N., and Nierhaus, K. H. (2006) The Highly Conserved LepA Is a Ribosomal Elongation Factor that Back-Translocates the Ribosome. *Cell 127*, 721–733.
15. Eymann, C., Homuth, G., Scharf, C., and Hecker, M. (2002) *Bacillus subtilis* functional genomics: Global characterization of the stringent response by proteome and transcriptome analysis. *J. Bacteriol. 184*, 2500–2520.
16. Qi, S. Y., Li, Y., Szyroki, A., Giles, I. G., Moir, A., and O'Connor, C. D. (1995) *Salmonella typhimurium* responses to a bactericidal protein from human neutrophils. *Mol. Microbiol. 17*, 523–531.
17. Barker, H. C., Kinsella, N., Jaspe, A., Friedrich, T., and O'Connor, C. D. (2000) Formate protects stationary-phase *Escherichia coli* and *Salmonella* cells from killing by a cationic antimicrobial peptide. *Mol. Microbiol. 35*, 1518–1529.
18. óvarsson, A., Brazhnikov, E., Garber, M., Zheltonosova, J., Chirgadze, Y., al-Karadaghi, S., Svensson, L. A., and Liljas, A. (1994) Three-dimensional structure of the ribosomal translocase: Elongation factor G from *Thermus thermophilus*. *EMBO J. 13*, 3669–3677.
19. Czworkowski, J., Wang, J., Steitz, T. A., and Moore, P. B. (1994) The crystal structure of elongation factor G complexed with GDP, at 2.7 Å resolution. *EMBO J. 13*, 3661–3668.
20. al-Karadaghi, S., Aevarsson, A., Garber, M., Zheltonosova, J., and Liljas, A. (1996) The structure of elongation factor G in complex with GDP: Conformational flexibility and nucleotide exchange. *Structure 4*, 555–565.
21. Evans, R. N., Blaha, G., Bailey, S., and Steitz, T. A. (2008) The structure of LepA, the ribosomal back translocase. *Proc. Natl. Acad. Sci. U.S.A. 105*, 4673–4678.
22. Zheng, L., Baumann, U., and Reymond, J. L. (2004) An efficient one-step site-directed and site-saturation mutagenesis protocol. *Nucleic Acids Res. 32*, e115.
23. Spedding, G. (1990) Isolation and analysis of ribosomes from prokaryotes, eukaryotes and organelles. In Ribosomes and protein synthesis: A practical approach (Spedding, G., Ed.) pp 5−8, IRL Press, New York.
24. McKinney, J., Guerrier-Takada, C., Gala, J., and Altman, S. (2002) Tightly Regulated Gene Expression System in *Salmonella enterica* Serovar Typhimurium. *J. Bacteriol. 184*, 6056–6059.

25. Neidhart, R. C., Bloch, P. L., and Smith, D. F. (1974) Culture medium for enterobacteria. *J. Bacteriol. 119*, 736–747.
26. Tosa, T., and Pizer, L. I. (1971) Biochemical basis for the antimetabolite action of L-serine hydroxamate. *J. Bacteriol. 106*, 972–982.
27. Cashel, M., Gentry, D. M., Hernandez, V. J., and Vinella, D. (1996) The stringent response. In Escherichia coli and Salmonella typhimurium: Cellular and Molecular Biology (Neidhardt, F. C., Ed.) Vol. 1, pp 1458−1496, American Society for Microbiology, Washington, DC.
28. Jain, V., Kumar, M., and Chatterji, D. (2006) ppGpp: Stringent response and survival. *J. Microbiol. 44*, 1–10.
29. Daigle, D. M., and Brown, E. D. (2004) Studies of the interaction of *Escherichia coli* YjeQ with the ribosome *in vitro*. *J. Bacteriol. 186*, 1381–1387.
30. Lanzetta, P. A., Alvaez, L. J., Reinach, P. S., and Candia, O. A. (1979) An improved assay for nanomole amounts of inorganic phosphate. *Anal. Biochem. 100*, 95–97.
31. Wang, L., and Brown, S. J. (2006) BindN: A web-based tool for efficient prediction of DNA and RNA binding sites in amino acid sequences. *Nucleic Acids Res. 34*, W243–W248.
32. Terribilini, M., Sander, J. D., Lee, J. H., Zaback, P., Jernigan, R. L., Honavar, V., and Dobbs, D. (2007) RNABindR: A server for analyzing and predicting RNA-binding sites in proteins. *Nucleic Acids Res. 35*, W578–W584.
33. Altschul, S. F., Madden, T. L., Schäffer, A. A., Zhang, J., Zhang, Z., Miller, W., and Lipman, D. J. (1997) Gapped BLAST and PSI-BLAST: A new generation of protein database search programs. *Nucleic Acids Res. 25*, 3389–3402.
34. Fiser, A., and Sali, A. (2003) Modeller: Generation and refinement of homology-based protein structure models. *Methods Enzymol. 374*, 461–491.
35. Martemyanov, K. A., Yarunin, A. S., Liljas, A., and Gudkov, A. T. (1998) An intact conformation at the tip of elongation factor G domain IV is functionally important. *FEBS Lett. 434*, 205–208.
36. Wriggers, W., Agrawal, R. K., Drew, D. L., McCammon, A., and Frank, J. (2001) Domain motions of EF-G bound to the 70S ribosome: Insights from a hand-shaking between multi-resolution structures. *Biophys. J. 79*, 1670–1678.
37. Møller, A. K., Leatham, M. P., Conway, T., Nuijten, P. J., de Haan, L. A., Krogfelt, K. A., and Cohen, P. S. (2003) An *Escherichia coli* MG1655 lipopolysaccharide deep-rough core mutant grows and survives in mouse cecal mucus but fails to colonize the mouse large intestine. *Infect. Immun. 71*, 2142–2152.
38. Wilson, K. S., and Noller, H. F. (1998) Mapping the position of translational elongation factor EF-G in the ribosome by directed hydroxyl radical probing. *Cell 92*, 131–139.
39. Agrawal, R. K., Heagle, A. B., Penczek, P., Grassucci, R. A., and Frank, J. (1999) EF-G-dependent GTP hydrolysis induces translocation accompanied by large conformational changes in the 70S ribosome. *Nat. Struct. Biol. 6*, 643–647.
40. Stark, H., Rodnina, M. V., Wieden, H. J., van Heel, M., and Wintermeyer, W. (2000) Large-scale movement of elongation factor G and extensive conformational change of the ribosome during translocation. *Cell 100*, 301–309.
41. Connell, S. R., Takemoto, C., Wilson, D. N., Wang, H., Murayama, K., Terada, T., Shirouzu, M., Rost, M., Schüler, M., Giesebrecht, J., Dabrowski, M., Mielke, T., Fucini, P., Yokoyama, S., and Spahn, C. M. (2007) Structural basis for interaction of the ribosome with the switch regions of GTP-bound elongation factors. *Mol. Cell 25*, 751–764.
42. Martemyanov, K. A., and Gudkov, A. T. (1999) Domain IV of elongation factor G from *Thermus thermophilus* is strictly required for translocation. *FEBS Lett. 452*, 155–159.
43. Savelsbergh, A., Matassova, N. B., Rodnina, M. V., and Wintermeyer, W. (2000) Role of domains 4 and 5 in elongation factor G functions on the ribosome. *J. Mol. Biol. 300*, 951–961.
44. DeLano, W. L. (2002) The PyMOL Molecular Graphics System, DeLano Scientific, San Carlos, CA.